18th International Conference on Space Operations, Montreal, Canada, 26 - 30 May 2025.

SpaceOps-2025, ID # 616

Design and Analysis of the Moonraker Spacecraft for Lunar LiDAR Mapping

Gregory Jovanovic[a]*, Brad Cotten[a], Robert Zee[a], Jesse Eyer [b], Kristian Damkjer [b], Hauke Hussmann[c], Klaus Gwinner [c], Konrad Willner [c]

[a] *SFL Missions Inc., 5000 Yonge Street, Suite 1901, Toronto, Ontario, Canada*, gjovanovic@sflmissions.com
[b] *NUVIEW GmbH, Prinz-Handjery-Str. 4, 14167 Berlin, Germany.* jesse@nuview.space
[c] *DLR Institute of Planetary Research, Rutherfordstr. 2, 12489 Berlin, Germany.* hauke.hussman@dlr.de
* Corresponding Author

Abstract

With renewed interest in lunar exploration, there is an increasing demand for high-resolution elevation maps of the Moon. Understanding the topography of the lunar south pole is crucial, as this region is a primary target for missions such as Artemis and CLPS. Unlike the mid-latitudes explored by the Apollo missions, the terrain near the south pole is extremely rugged, making landing site selection challenging. While NASA's Lunar Reconnaissance Orbiter has provided the best topographic data available, there are gaps and insufficient resolution to effectively mitigate landing risks.

The Moonraker mission will address these challenges with a LiDAR-based mapping instrument to significantly enhance the resolution of lunar topographic maps, providing mission planners with the tools necessary to identify and assess future landing sites. Operating in a low lunar orbit, the Moonraker small satellite will employ a 1X zoom mode to produce wide-area 3D maps of the Moon's polar regions with a 4-meter ground sample distance. The 8X zoom mode will improve resolution, enabling the detection of potential landing hazards. Additionally, Moonraker's LiDAR data will serve a broader scientific purpose, including scanning permanently shadowed regions for water ice and providing valuable insights into the Moon's geological and interior composition.

Key aspects of the mission profile and design have been established and are presented. Through comprehensive analysis and trade studies, trajectory options for the lunar transit and operational orbits at the Moon are evaluated, with the optimal selections identified. The science objectives are elaborated and their impact on payload and spacecraft requirements is discussed. The thermal and radiation environments that the spacecraft will experience are defined. Preliminary work on the spacecraft system design is presented, with analysis on communication links, power generation, and the navigation approach.

Moonraker is currently in a Pre-Phase A study, funded by the European Space Agency within a new initiative on Small Missions for Exploration, and its inception "Destination the Moon". The project consortium includes six organizations: NUVIEW GmbH (the prime contractor responsible for the LiDAR payload), SFL Missions Inc. (responsible for the spacecraft bus and system integration), DLR's Institute of Planetary Research (which will process the LiDAR data and develop the elevation maps), along with additional partners Lunar Outpost EU, AEM Antennas Inc., and KSAT, who will contribute to the design, development, and operation of Moonraker. Collaboration between the consortium members is essential and a single-source-of-truth approach will be followed using MBSE modelling to help achieve mission success.

Keywords: Lunar exploration, LiDAR-based mapping, small satellite, mission analysis, systems design

Acronyms/Abbreviations

CLPS	Commercial Lunar Payload Service
DEM	Digital Elevation Map
EKF	Extended Kalman Filter
EML1	Earth-Moon L1
ESA	European Space Agency
GSD	Ground Sampling Distance
GTO	Geostationary Transfer Orbit
HDA	Hazard Detection and Avoidance
LEO	Low Earth Orbit
LiDAR	Light Detection and Ranging
LOI	Lunar Orbit Insertion
LOLA	Lunar Orbiter Laser Altimeter
LRO	Lunar Reconnaissance Orbiter
LV	Launch Vehicle
NASA	National Aeronautics and Space Administration
QF	Quasi-Frozen
SFL	Space Flight Laboratory
SPENVIS	SPace ENVIronment Simulator
TID	Total Ionizing Dose
TLI	Trans-Lunar Injection
TT&C	Telemetry, Tracking, and Command
WSB	Weak Stability Boundary

1. Introduction

As the ISS reaches the end of its design life, the focus of manned and robotic space exploration has returned to the Moon. The Chinese, Indian, and Japanese governments have all launched lunar landers within the past decade, while CLPS missions from the US, and other commercial missions from Israel and Japan, have begun launching with increased frequency. Furthermore, starting later this decade, the Artemis program plans to return mankind to the Moon for the first time in over 60 years, while construction of the Gateway space station will also commence, leading to humanity's first permanent outpost in lunar space.

Significant attention has been focused on the Moon's south pole as a region for exploration. Here, permanently shadowed craters could hold volatiles such as water ice, a key resource to support long-term human habitation on the Moon. As well, permanently sun-lit crater rims and massifs offer extensive solar power generation potential to landers and future lunar bases. But unlike the gentler, mid-latitude regions explored by Apollo, the topography of the Moon's South Pole is extremely rough. This presents a challenge for mission planners who generally need to select landing sites near targets of exploration (e.g. deep craters and tall mountains), but need to prioritize lander safety. As recent lunar lander missions have shown, tipping over on slopes or landing site hazards, such as boulders or small craters, is a very real risk. This risk becomes unacceptable for manned landers where astronaut lives are on the line.

Currently, the best topographical data available to mission planners comes from NASA's Lunar Reconnaissance Orbiter (LRO). It's main payload, the Lunar Orbiter Laser Altimeter (LOLA) has mapped the Moon's surface in 3D since 2009 and has produced stunning digital elevation models (DEMs) of the lunar surface. However, with its small laser spot size (5 m) and long pulse length (5 nm FWHM), the LRO data has significant gaps. It provides a vertical precision of 20 cm, and a horizontal resolution of 20 m ground sampling distance (GSD). This is insufficient coverage and resolution to identify hazards in prospective landing sites. Modern landers therefore have a choice of landing blindly and risking tip-over hazards, or performing a hover maneuver over the landing site and scanning it with a hazard detection and avoidance (HDA) LiDAR. If no flat and obstacle-free area can be found, the lander must carry sufficient propellant to divert to one or two alternative landing sites and perform additional HDA scans. This method carries a substantial risk that no safe landing site will be found.

To address the current limitations, the Moonraker spacecraft is proposed. Moonraker will use a LiDAR instrument to identify and de-risk landing sites for future lunar lander missions. The instrument's 1X zoom mode will generate

wide-area 3D maps of the Moon's polar regions to aid in landing site selection, while the 8X zoom mode will identify and characterize potential hazards at those landing sites in unprecedented detail.

For the Moonraker LiDAR instrument to perform its objectives at the Moon, it needs a spacecraft uniquely developed to survival the lunar environment and meet the technical challenges of such a mission. Lunar orbiters must be designed for different scenarios than Earth orbiting spacecraft which include completing the transit to the Moon and performing a capture maneuver into a stable lunar orbit. Today, there are more trajectories being used to reach the Moon which allow the spacecraft to use different types of propulsion systems. While in orbit about the Moon, the lumpy lunar gravitational field will perturb the orbit of the spacecraft and require more regular orbit maintenance, especially at lower altitudes, when compared to the Earth. Other technical challenges include increased radiation dosage, more challenging thermal environments, long distance communication links, orbit determination, and more.

2. Science Objectives

With plans for re-establishing human presence on the Moon within this decade, lunar exploration is of key importance in planetary research. Two main aspects, safety for the astronauts and scientific exploration of the Moon, are therefore major drivers for Moonraker.

The primary scientific objective for Moonraker will be to provide enhanced mapping of the polar regions that will significantly improve the density of topographic data points to characterize candidate landing sites in more detail with the goal of minimize risks for human and robotic exploration. Studies will include elevation variation, slope distribution, and boulder distribution within the selected areas across baselines as small as 0.5 m.

Furthermore, Moonraker's data will enhance the knowledge of illumination and thermal conditions and in addition will help provide insights into ice deposits by measuring the surface [1]. With its dense, highly precise height information collected over a longer time span, Moonraker will provide the required dataset to determine the precise orientation of the lunar rotational axis which has implications on the physical properties at the surface, regarding time-variable thermal conditions. The expected data will also support the refinement of the libration amplitudes and phases in longitude and latitude, which depend on the lunar moments of inertia and therefore contain information on the deep lunar interior. By observing periodic changes in the degree-two shape, the tidal deformation on the main tidal cycle of 27 days could potentially be detected. Depending on the actual amplitude, which is currently unknown, this will provide constraints on the rheology and dissipation of the lunar interior.

Lastly, the precise topographic data-set allows insight into understanding the of magmatic history of the Moon, measure small impact create sizes to assess the recent impact rate, determine recent crustal deformation for insight into lunar tectonics, study the dynamics of mass wasting event on the Moon, and understand the evolution of the lunar regolith.

3. Payload Overview

The payload for Moonraker is a LiDAR system that uses a near-infrared laser to perform altitude measurements that are converted into digital elevation maps of the lunar surface. The transmitter optics use a refractive beam expander sized to achieve the desired beam divergence. A selectable diffractive optical element will allow the beam to switch between a 1 km wide laser swath, for the 1X zoom mode, and a 125 m swath, for the 8X zoom mode. A fast scanning mirror will control the beam's path, sweeping the laser footprint back and forth across the transmit telescope's field of view.

The payload includes two receive telescopes, one for the 1 km wide swath and the other for the 125 m wide swaths. The telescopes use refractive optics since the sensor cannot support two drastically different zoom modes. The 1X zoom receive telescope has a 78 mm aperture to provide the 4 m GSD and the 8X zoom telescope has a 150 mm aperture for the 0.5 m GSD. The camera used to capture the incoming photons a 128 x 32 pixel sensor. The sensor must remain cold during operation and a thermal electric cooler is used to maintain this cool temperature. The system is controlled by the payload avionics which includes its own power regulation and distribution system, payload command routing, telemetry collection for all units, along with a precise clock to synchronize the laser, sensor and the rest of the payload components. The payload will also require heaters during nominal operations when not actively scanning to keep the components within their operating temperatures, and survival heaters to keep the units within

their non-operational temperatures when the payload is off. An overview of the payload specifications is provided in Table 1.

Table 1. Moonraker LiDAR Specifications and Performance Metrics

Parameter	Value
Mass	51.2 kg
Average Power	251.1 W
Peak Power	486.4 W
Duty Cycle per Orbit	30%
1X Zoom Cell Size	4 m
8X Zoom Cell Size	0.5 m
Points per Cell	2
1X Zoom Swath Width x Length	1 x 3275 km
8X Zoom Swath Width x Length	425 x 425 m

The 1X and 8X zoom modes for the LiDAR payload will have separate coverage goals during the mission. The 1X mode will perform wide area scanning at 4 m GSD, while the 8X mode will be used solely to obtain high resolution scans of small areas of interest of 425 x 425 m. A coverage study was performed, with the 1X zoom mode, to determine the duty cycle of the payload that would maximize the science goals of the mission without over complicating the design. To help inform this decision, the data generation rate, coverage rate, surface area to scan, and downlink time are considered. The LiDAR payload has an effective swath width of 900 m, 10% of the 1 km swath is used to overlap with other scans for data co-registration, which results in a coverage rate is 2.70×10^7 m^2/s. Therefore, to scan the two polar regions, each with an area of 2.54×10^{12} m^2, it would take 2.3 years with a payload duty cycle of 10% and 0.8 years with 30%. To scan the entire lunar surface, it would take 17.1 and 5.7 years with a 10% and 30% payload duty cycle respectively. By using a 30% duty cycle, this would help the mission complete its primary objective of mapping both polar regions within the first year of payload operations. The design changes to the spacecraft are minor to allow the payload to operate at a 30% duty cycle and would only require a slightly larger deployable solar arrays and higher capacity battery pack. Therefore, the payload duty cycle duty cycle will be 30% for the Moonraker mission as it enables the spacecraft to scan a significantly greater portion of the Moon within the same time frame and only requires minor changes to the spacecraft design.

4. Platform Overview

Moonraker will use SFL's DAUNTLESS-L platform, a lunar version of the existing DAUNTLESS platform. This lunar version is currently under development and will be available for Moon missions prior to the implementation phase for Moonraker. This platform is intended for spacecraft with a total mass up to 600 kg, using a 24-inch diameter ring or a 4-point release system launch interface. The spacecraft will use a standard design with heritage components for command & data handling, power management, navigation, and attitude control. Certain subsystem hardware is sized/selected based on the power, pointing, propulsion, and data throughput requirements for the mission. A summary of the performance and characteristics for the proposed spacecraft is provided in Table 2 below.

Table 2. Moonraker Spacecraft Performance Metrics and Design Characteristics

Parameter	Value
Spacecraft Dry Mass	259 kg
Propellant Mass	Primary Propulsion System: 213 kg Reaction Control System: 6 kg
Spacecraft Wet Mass	478 kg
Spacecraft Dimensions	Stowed: 1.35 m x 1.10 m x 1.39 m Deployed: 1.35 m x 1.10 m x 5.49 m
Peak Power Generation (end-of-life)	697 W
Platform Data Storage	Telemetry: 2 GB Payload Data: 256 GB
Omnidirectional (Safehold) Telemetry & Command Link	Uplink: 4 kbps (fixed) Downlink: 0.25 to 16 kbps (adjustable)
Directional Telemetry & Command Link	Uplink: Up to 2 Mbps (adjustable) Downlink: Up to 2 Mbps (adjustable)
Payload Data Downlink	Up to 200 Mbps (adjustable, limited by link budget)
Attitude Determination	7.9 arcsec (1σ, nadir, not including static and thermal misalignments)
Attitude Control	9.6 arcsec (1σ, nadir, not including static and thermal misalignments)
Pointing Agility (peak slew rate)	0.4 °/s
Delta-V	1453 m/s
Design Life	5 years
Power Generation	2 deployable solar arrays, 6 keep-alive panels
Battery	49.6 A·h capacity battery pack
Bus Voltage	28 V unregulated
Communications	Omnidirectional Telemetry & Command: X-band Directional Telemetry & Command: X-band Payload Data Downlink: Ka-band
Attitude Determination	3-axis; 2x star tracker, 6x sun sensor, rate sensor
Attitude Control	3-axis; 4x reaction wheels, 8x reaction control thrusters
Navigation	Two-way Doppler and two-way ranging
Propulsion & Reaction Control System (RCS)	Monopropellant primary thrusters Cold gas RCS thrusters

5. Lunar Trajectory Analysis

As spaceflight has matured, different trajectory options have been discovered leading to a variety of potential pathways to the Moon. At first, direct lunar transfers were performed using high thrust engines that would put the spacecraft onto a Hohmann transfer such that its apoapsis would meet with the Moon where it would perform a high impulse lunar orbit insertion (LOI) maneuver to capture into lunar orbit. A simulation of this trajectory is shown in Fig. 1. The trajectory begins on January 1, 2029 and a trans-lunar injection (TLI) maneuver is simulated by the launch vehicle (LV). The spacecraft reaches the Moon 5 days later and performs the lunar orbit insertion maneuver by applying 340 m/s of delta-V with a 25 minute burn time. This maneuver captures the spacecraft into a stable lunar polar orbit with a periapsis altitude of 200 km and an apoapsis altitude of 8600 km. Next, the spacecraft performs 5 successive

burns at periapsis for 5.7 minutes each to circularize the orbit and complete the descent to the operational low lunar orbit.

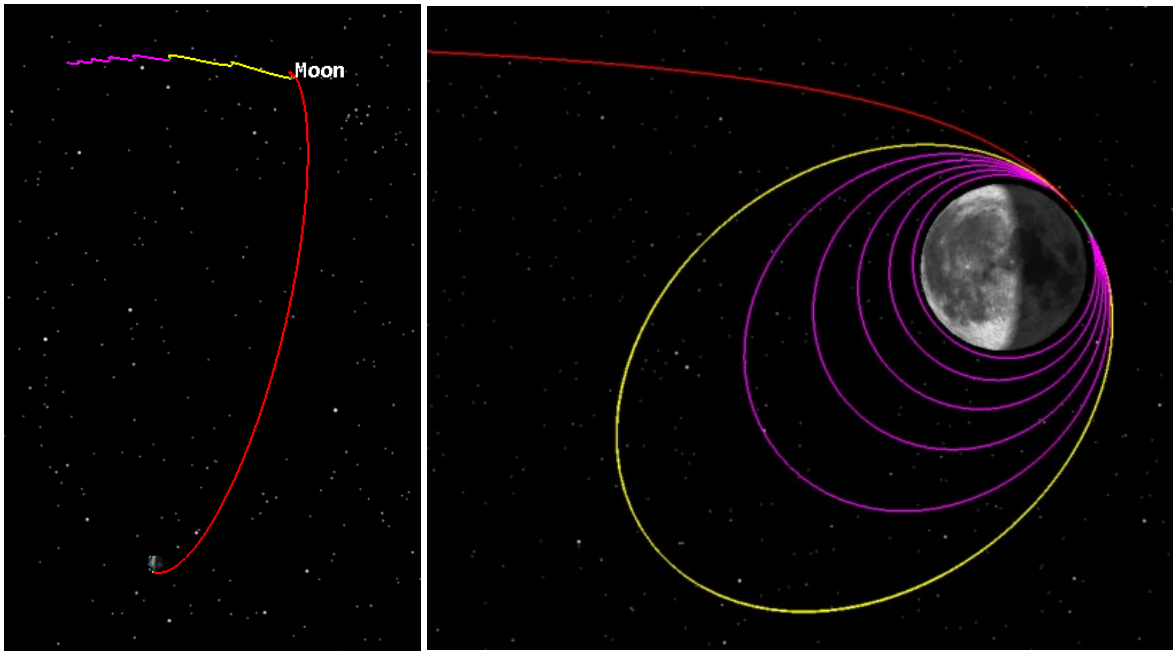

Fig. 1. A Simulation in STK of the Direct Transfer Lunar Trajectory

Later, ballistic transfer trajectories were discovered that made use of the weak stability boundary (WSB) in the three and four body problem that uses invariant manifolds as pathways to libration points and lunar orbits [2]. These ballistic transfers require an injection with a high thrust engine but can be captured at libration points with no LOI maneuver required and in general require less delta-V than a direct lunar transfer. A final lunar transfer method has been demonstrated with ESA's SMART-1 mission that used a low thrust propulsion system [3]. In the restricted three body problem, unique orbits exist around the libration points which include transit orbits that will take a spacecraft from an orbit about one body to another. SMART-1 made use of the Earth-Moon L1 (EML1) transfer orbit to reach the Moon. A simulation of this trajectory is shown in Fig. 2. These three trajectories were analyzed to determine the best option for the Moonraker spacecraft.

The simulation begins on June 13, 2028 from a geostationary transfer orbit (GTO) (250 x 36,000 km altitude). The spacecraft continuously uses its engines in a spiral trajectory to escape the lower Van Allen belt and achieves a 20,000 x 80,000 km orbit on August 11, 2028 (59 days later). After this, the apoapsis is raised strategically until the spacecraft crosses the Lagrange point on January 1, 2029. After coasting to the first periapsis about the Moon, the spacecraft uses its propulsion system to reduce its speed to help it enter into a stable lunar orbit. The trajectory phase ends when the spacecraft reaches a 100 x 100 km altitude on March 18, 2029 (278 days since the first engine firing).

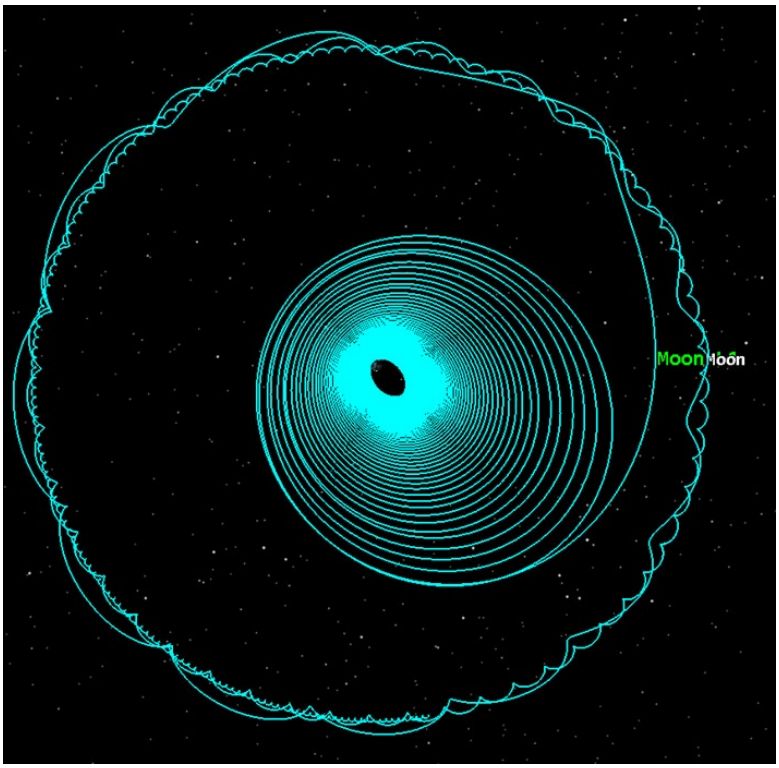

Fig. 2. A Simulation in STK of the Earth-Moon L1 Transfer Trajectory in the Earth Rotating Frame

When comparing the two high thrust trajectories, the ballistic transfer method requires slightly less propellant than the direct transfer. This would help to reduce the launch cost by reducing propellant, but it is unlikely to have a large effect on the propellant tank volume and the overall size and dry mass of the structure. The ballistic transfer maneuver is much more complex than the direct transfer method and requires more complex analysis and maneuver planning leading to greater mission risk. The ballistic transit duration is significantly longer than a direct transfer trajectory which will slightly worsen the radiation exposure and the thermal environment but eliminates the time critical commissioning required during the 4 to 6 day transit of a direct transfer. A ballistic transfer will reduce the launch mass of the spacecraft, but the additional fuel required for the trans-lunar injection performed by the launch vehicle may offset any cost savings. The overall design of the spacecraft will not change drastically between either option so the hardware and testing will be similar leading to almost identical spacecraft costs. Due to the more complex maneuver required, longer transit duration, and more risk closing some of the subsystems, the direct lunar transfer trajectory provides a better option than the ballistic transfer for Moonraker.

Next, the direct transfer and the EML1 transfer are compared. The biggest advantage of the EML1 trajectory a 100 kg reduction in propellant due to the use of an electric propulsion system. This would drastically reduce the launch cost for this mission. However, the dry mass for the direct transfer ends up being smaller, even though it carries more propellant mass, due to the smaller solar arrays, battery, and less radiation shielding as it would only pass through the Van Allen belts once. The direct transfer trajectory is much more straightforward from an operations and complexity standpoint than the low thrust EML1 trajectory. The spacecraft is just responsible for a maneuver to capture at the Moon and to lower the altitude over a few orbits, whereas the low thrust trajectory can take up to 15 months of constant maneuvers. Lastly, the spacecraft and subsystem design are simpler using a high thrust trajectory as the high power demand from the electric propulsion system is not required and the spacecraft does not require as much radiation shielding. Therefore, the direct lunar transfer trajectory was selected for Moonraker.

6. Operational Orbit Analysis

The mass distribution throughout the Moon is not as uniform compared to Earth, which leads to a lumpy gravitational field that causes larger orbital perturbations. The perturbations at the Moon are generally one order of magnitude larger than at the Earth [4] but become smaller in higher altitude orbits. These large perturbations necessitate

orbital station keeping in the majority of lunar orbits. Despite these perturbations, there are specific orbits about the Moon which have constant orbital elements and are known as frozen lunar orbits and equations of motion defining these orbits can be derived [5]. However, there are no frozen polar orbits, and Moonraker requires a polar orbit in order to fulfill its primary science objectives.

The same analysis performed to calculate the conditions for frozen orbits results in equations describing the rate of change of each orbital element. Using these rate of change equations, quasi-frozen (QF) orbits can be constructed where the variation of orbital elements follows a cyclic pattern every lunar sidereal period (approximately 27.3 days) with minimal drift. In this same analysis, the rate of change for each orbital element is derived and the elements with the highest drift rate are the argument of periapsis and eccentricity [5]. Quasi-frozen orbits have been used for various mission such as LRO for commissioning and its mission extension to help reduce the propellant consumption for station keeping maneuvers and can prolong the mission life of a satellite orbiting around the Moon.

For the Moonraker spacecraft, a low altitude orbit is required to achieve a high photon density for high resolution digital elevation maps and a 50 km altitude target is set. Two orbits were analyzed, a 50 km altitude circular polar orbit and a 30 x 181.5 km polar orbit with its periapsis at 270°. These orbits were simulated in STK and the altitude, and argument of periapsis for the quasi-frozen orbit, drift was measured. To propagate the orbit about the Moon, the "Moon High-Precision Orbit Propagator Default v10" built into STK is used. For the circular orbit, an orbit maintenance is performed once per sidereal period which brings the orbit back to a circular 50 km altitude. This results in a total of 13 station keeping events over a year with each event using 10.1 m/s of delta-V. The altitude drift with station keeping maneuvers for the 50 km circular orbit is shown in Fig. 3.

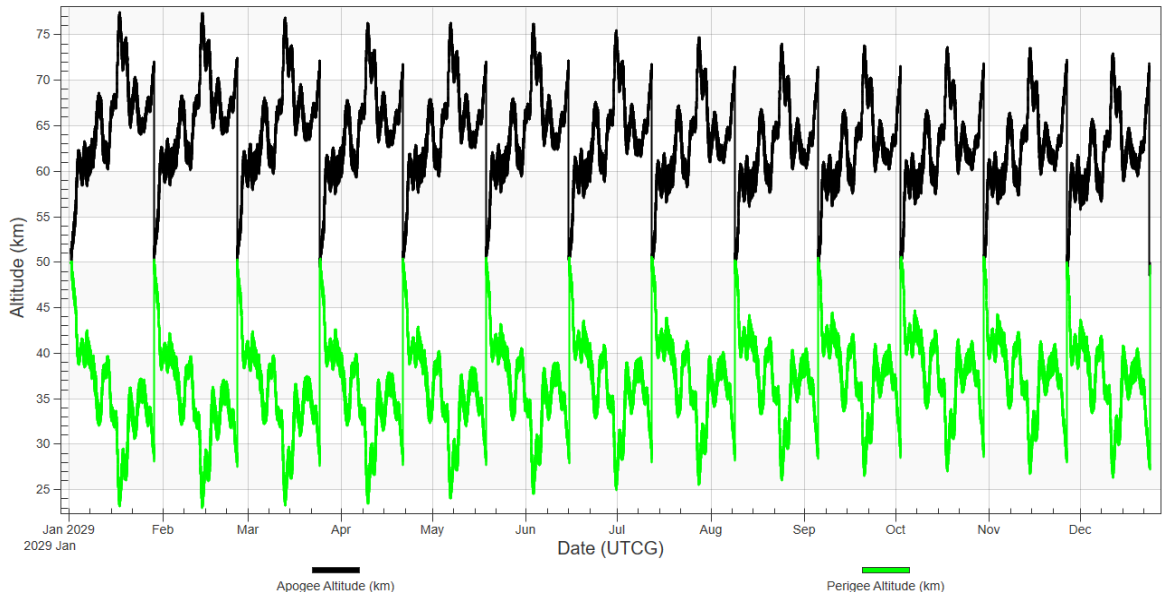

Fig. 3. Periapsis and Apoapsis Drift in a 50 km Circular Polar Orbit over a Year with Station Keeping Maneuvers

A quasi-static orbit was found in STK such that the orbit was sufficiently stable over 13 sidereal periods. This orbit is centered about the south pole and has an initial periapsis and apoapsis altitudes of 30 x 181.5 km. During the 13 sidereal periods, the argument of periapsis stays bounded within +/- 10° and the periapsis altitude varies between 15 and 50 km. The maximum altitude within the south pole region is only 60 km. At the end of the 13 sidereal period, the spacecraft performs a maneuver using 76 m/s of delta-V to move its argument of periapsis to the north pole to begin scanning that region. The results from the year-long simulation of the quasi-frozen orbit are shown in Fig. 4.

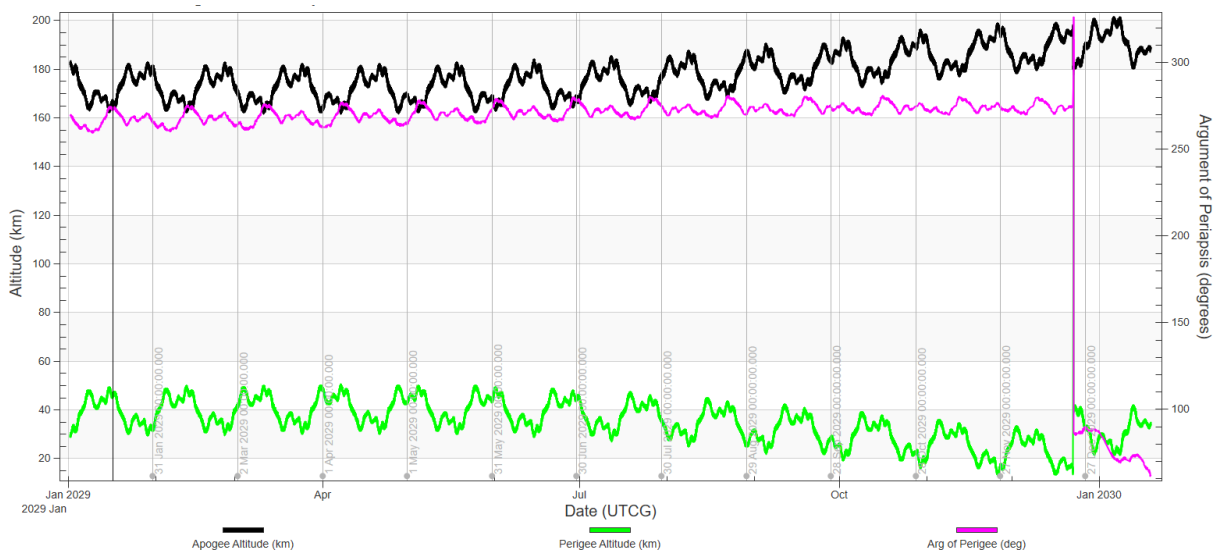

Fig. 4. Altitude and Argument of Periapsis Drift over a Year with an Orbit Reset to the North Pole for a 30 x 181.5 km Quasi-Frozen Orbit

The major benefit of the quasi-frozen orbit is the reduction in propellant mass since its orbit is stable over a year and only requires a maneuver to reset the quasi-frozen orbit whereas the circular orbit requires station keeping maneuvers once every sidereal period, which adds up to more total delta-V expended. The delta-V reduction, and the small reduction in dry mass due to a smaller structure, results in a total mass savings of 33 kg. The drawbacks of the quasi-frozen orbit include increased payload complexity, more variation of orbital element drift and altitude within the pole region, and more challenging operations. The altitude of periapsis in a low lunar circular orbit will drift lower by 20 to 25 km whereas the periapsis altitude of a quasi-frozen orbit fluctuates by +/- 15 to 20 km and can reach higher altitudes near the edge of the polar region. To scan the polar region in a quasi-frozen orbit, the payload must accommodate a wider range of altitudes and faster speeds as the spacecraft is moving more quickly at the periapsis for elliptical orbits.

The quasi-frozen orbit can be beneficial to reduce the spacecraft mass and launch costs along with reducing the number of station keeping maneuvers, but will make the design and operation of the payload more complicated. Based on the trade study, the launch cost savings are relatively small and do not outweigh the added payload complexity. Therefore, a polar circular orbit with an altitude of 50 km is selected as the operational orbit for Moonraker.

7. Moonraker Concept of Operations

The Moonraker spacecraft is designed to operate in a set of modes that fulfill different aspects of the mission. The spacecraft modes include: Safehold, Detumble, Standby, Earth Communications, and Tracking, Maneuvering, and Payload Operations.

Safehold mode is used after launch vehicle separation and in the event of any anomalies. Only essential hardware is powered and attitude control is not available. Worst-case power generation is assumed, and survival heaters are used to maintain the temperature of the payload and critical components. Detumble mode is used during commissioning or after recovering from safehold to eliminate spacecraft angular rates. Survival heaters are used to maintain the temperature of the payload and critical components. Standby mode is the default state when spacecraft is in nominal conditions and not performing any payload operations, communication or ranging, or maneuvers. The spacecraft will perform sun tracking while and momentum management in this state.

Earth Communications and Tracking mode involves pointing the spacecraft high gain antenna towards Earth for communications and ranging. This mode enables the downlink of payload data over Ka-band, and X-band will be used to perform ranging, telemetry downlink, upload of time tagged commands, and to update on-board orbit parameters. Maneuvering mode is used to perform any impulses to adjust the trajectory or orbit of the spacecraft. The mode includes any necessary initialization of the propulsion subsystem including pre-heating, as well as setting the spacecraft

attitude to achieve the desired thrust vector before executing the impulse. Payload Operations mode will support the LiDAR scanning operations. In this mode the payload aperture will be pointed towards the surface of the Moon. The payload radiator and star trackers will be orientated towards deep space such that the Sun, Earth, and lunar limb stays outside of the star tracker field of views.

A typical orbit during operations around the moon will be begin in Standby mode. Before the spacecraft reaches an area of interest, the spacecraft will shift into Payload Operations mode to prepare for and scan the ground target. The spacecraft will return to Standby mode and wait for the next scheduled ground contact. The spacecraft will enter Earth Communications and Tracking mode to prepare for the contact, where newly acquired payload data will be downlinked. The spacecraft will again return to Standby mode, and this sequence will repeat each orbit.

The payload will produce 5.13 GB of data with a 30% duty cycle and with the payload downlink data rate of 200 Mbps the downlink time per orbit would be 3.7 minutes. However, the spacecraft will only perform Earth communications a few times a day resulting in a 12% duty cycle over an orbit. The remainder of the orbit will be in Standby mode. A summary of the duty cycle for each spacecraft mode during nominal operations is shown in Table 3.

Table 3. Duty Cycle for Each Spacecraft Mode During Nominal Operations

Spacecraft Mode	Orbit Duty Cycle [%]
Payload Operations	30
Earth Communications and Tracking	12
Standby	58

At end-of-life for Moonraker, ESA standard ESSB-ST-U-007 will be followed to responsibly dispose of the spacecraft. This standard specifies that a spacecraft in lunar orbit at the end of its mission shall be put into a heliocentric orbit or impact into the Moon [6]. Since Moonraker is in a low altitude orbit, it can perform a 12 m/s burn to cause the spacecraft to impact the Moon.

8. Lunar Environment

The lunar orbital environment presents many more challenges for spacecraft than when orbiting at the Earth, especially in low Earth orbits (LEO). This is seen in the inconsistent thermal environment and more intense radiation.

1.1 *Thermal Environment*

The thermal environment in a circular 50 km altitude polar low lunar orbit was assessed. In lunar orbit, the lunar IR and albedo, along with the solar flux, must be considered as thermal loads the spacecraft will experience. As the position of the Moon changes relative to the Sun, the solar flux will vary between 1310 and 1426 W/m^2. The worst-case cold (WCC) scenario is when the Moon is the farthest away from the Sun and worst-case hot (WCH) is when it is the closest.

Since the Moon is tidally locked to the Earth, its rate of rotation about its axis causes it to make one full rotation every 27.3 Earth days; which causes the lunar IR flux to be greatest in the center of the sunlit portion of the Moon and drops off close to zero on the dark side of the Moon. The maximum instantaneous lunar IR on the sunlit side is between 1114 W/m^2 and 1335 W/m^2 depending on time of year, and the minimum on the dark side is 5 W/m^2 [7] The lunar IR heat flux will also vary due to the beta angle of the spacecraft. For a 0° beta angle the spacecraft will pass over the center of the sunlit side of the Moon resulting in the highest average lunar IR flux of 805 W/m^2 (for WCH) on the sunlit side and experience 5 W/m^2 on the dark side for a total orbit average of 405 W/m^2. A beta angle of 90° results in an average lunar IR flux of 5 W/m^2 as the spacecraft does not pass over the sunlit portion of the moon. The average lunar IR heat flux is summarized in Table 4.

Table 4. Lunar IR Heat Flux in Different Conditions

Beta Angle [°]	Sunlit Average [W/m^2]		Dark Side Average [W/m^2]		Orbit Average [W/m^2]	
	WCC	WCH	WCC	WCH	WCC	WCH
0	672	805	5	5	339	405
90	-	-	5	5	5	5

The lunar albedo varies between 0.07 and 0.20 based on the lunar surface composition [8]. In the WCC scenario, an albedo of 0.07 and solar flux of 1310 W/m^2 results in a maximum heat flux of 92 W/m^2; and in the WCH scenario, an albedo of 0.20 and solar flux of 1426 W/m^2 results in a maximum heat flux of 285 W/m^2.

For circular lunar orbits, the variation in thermal loads is studied and plotted for various orbit altitudes. Fig. 5 and Fig. 6 show the heat flux variation for an orbit with a beta angle of 0°. For a 0° beta angle, the average solar flux is lower at lower altitudes as the spacecraft spends a larger fraction of the orbit in eclipse. The average lunar IR and albedo flux act inversely to the solar flux and get lower as the altitude increases. For a 90° beta angle, there is little to no contribution from the lunar IR and albedo, and since the spacecraft does not enter eclipse, the average flux is simply equal to the solar flux. Overall, the coldest thermal environment occurs at the lowest altitude with a beta angle of 0°, and the hottest thermal environment occurs for a beta angle of 90° and is independent of orbit altitude.

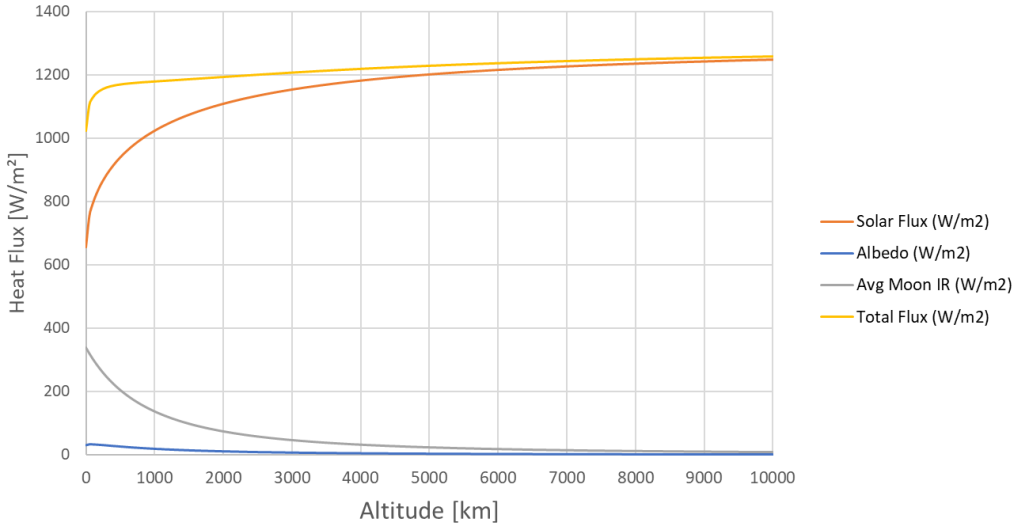

Fig. 5. Average Heat Flux vs. Circular Orbit Altitude (WCC and Beta Angle = 0°)

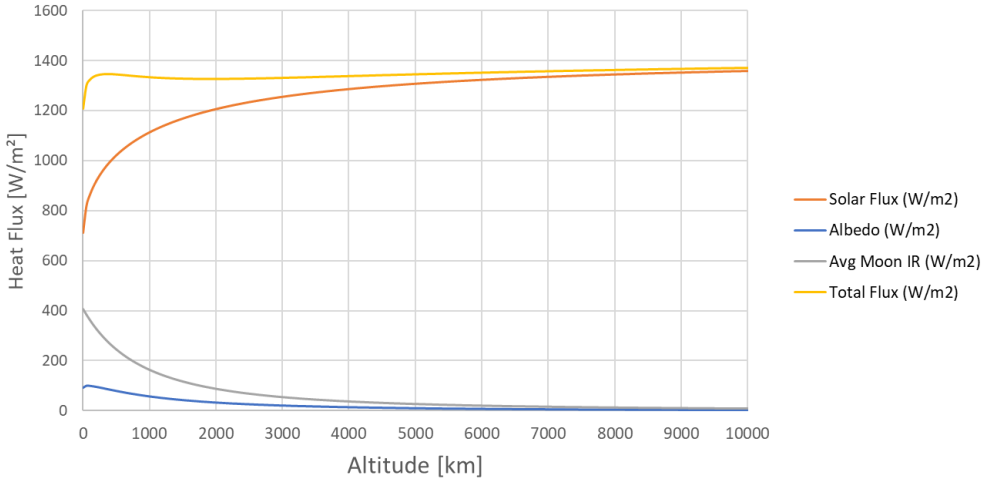

Fig. 6. Average Heat Flux vs. Circular Orbit Altitude (WCH and Beta Angle = 0°)

A similar analysis was performed for a 50 x 140 km altitude polar quasi-frozen orbit that will be used to commission the spacecraft before payload operations and in a 200 x 4000 km altitude polar orbit that the spacecraft will initially be captured into. The minimum and maximum heat fluxes for all orbits are shown in Table 5.

Table 5. Summary of the Maximum and Minimum Thermal Loads over Various Lunar Orbits

Orbit Altitude	Solar Flux [W/m^2]		Moon IR Flux [W/m^2]		Albedo Flux [W/m^2]		Total Flux [W/m^2]	
[km]	Min	Max	Min	Max	Min	Max	Min	Max
50 x 50	753	1426	5.0	382	0	99	758	1907
50 x 140	753	1426	4.2	382	0	99	727	1907
200 x 4000	846	1426	0.5	325	0	94	847	1845

From this investigation into the thermal environment during operations around the Moon, it was observed that the spacecraft could experience large temperature gradients, and very cold solar array temperatures. To address these thermal concerns, the spacecraft will employ multi-layer insulation to help isolate it from the external thermal environment. Heaters will also be used at strategic locations within the spacecraft platform and payload. The solar arrays will be designed for very cold temperatures, and these temperatures will be applied during solar array and spacecraft level testing.

1.2 Radiation Environment

The radiation Moonraker will experience is highly dependent on the trajectory it takes to get to the Moon and how long it stays in its operational orbit. Radiation can be harmful to a satellite as it can damage the electronics, cause hardware and software upsets, and will degrade the performance of solar cells. The radiation analysis is performed using SPace ENVIronment Simulator (SPENVIS). Within SPENVIS, the radiation environment can be simulated based on the trajectory and epoch of a spacecraft. The models used to simulate the radiation environment are outlined in Table 6. The total ionizing dose (TID) is determined for the various segments of the mission and the effect of solar cell degradation is analyzed using the SHIELDOSE-2 [9] model. The components for which TID is analyzed are idealized as a silicon medium at the center of an aluminum sphere of specified thickness.

Table 6. Radiation Source Models

Radiation Source	Model
Solar Protons/Heavy Ions	SAPPHIRE [10]
Galactic Cosmic Rays	CREME96 [11]
Trapped Protons	AP-8 [12]
Trapped Electrons	AE-8 [12]

Solar radiation is the continuous stream of subluminal ions, primarily protons and helium nuclei, and a small distribution of heavier atomic elements, radiated from the sun. This radiation source dominates the radiation environment for the majority of the mission, except when shielded by the Earth's magnetic field or when the Sun is eclipsed by the Earth or Moon. In Lunar orbit, solar radiation fluence is proportional to the percentage of time the spacecraft spends in direct sunlight throughout the year. The spacecraft is also shielded from Solar radiation once per lunation when the Moon enters the Earth's magnetotail, for which transits typically last a few days each month.

Galactic cosmic rays (GCR) are the secondary radiation source in deep space and represents the stream of subluminal charged particles that originate beyond our solar system but within the Milky Way galaxy. GCRs have a much lower particle flux than solar radiation, however the energy of each particle is generally much greater than solar radiation. The Moon blocks GCRs, proportionally to its angular diameter from the spacecraft. The Earth's magnetic field traps energetic charged particles in two main belts, known as the Van Allen belts. The inner belt has significantly higher fluence than the outer belt and poses a serious risk to spacecraft that spend extended periods in its domain. Both radiation belts become more intense with increasing solar activity, with the outer belt being more sensitive and the inner belt being more stable.

The various lunar transfer options, direct lunar transfer, ballistic transfer, and the EML1 transfer, were all simulated in SPENVIS to assess the TID for each trajectory. The results are shown in Fig. 7. Each scenario is calculated in a solar maximum and minimum and both are displayed on the plots for each trajectory. The shaded region between the solar min and max indicates the possible results for a given transfer method.

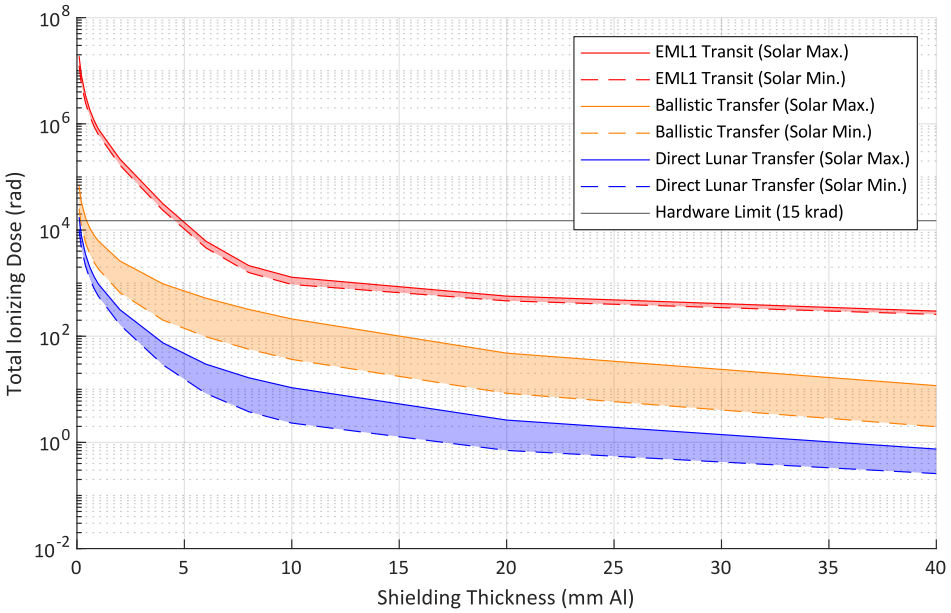

Fig. 7. Total Ionizing Dose for the Three Trajectory Options vs. Shielding Thickness

The EML1 transfer is an attractive option for utilization of highly efficient electric propulsion, at the expense of extended exposure to intense radiation induced by the trapped particles in the Van Allen radiation belts. Both the direct lunar transfer and ballistic transfer are attractive from a radiation standpoint, as the spacecraft only makes a single pass through the Van Allen belts.

Another disadvantage of the EML1 transit, is the advanced solar cell degradation due to extended exposure to the Van Allen belts. The 1 MeV equivalent dose of radiation to the spacecraft during the transfer exceeds 1015 e/cm^2, which exceeds the specified degradation for many commercially available solar cells. Preliminary analysis suggests the solar cells would experience up to 16% degradation in power generation from beginning-of-life values before entering lunar orbit. The degradation performance of typical triple-junction solar cells is presented in Table 7. The direct lunar transfer is not considered as there is effectively no solar cell degradation experienced during this transfer due to its short duration.

Table 7. Solar Cell Degradation for Lunar Transfers

Transfer Type	1 MeV Equivalent Flux [e/cm^2]			Degradation Factor		
	P_{max}	V_{OC}	I_{SC}	P_{max}	V_{OC}	I_{SC}
EML1 Transfer in Solar Min	1.29×10^{15}	3.25×10^{15}	6.98×10^{14}	0.877	0.926	0.987
EML1 Transfer in Solar Max	1.36×10^{15}	3.41×10^{15}	7.36×10^{14}	0.873	0.926	0.980
Ballistic Transfer in Solar Min	1.21×10^{13}	3.05×10^{13}	6.53×10^{12}	0.998	0.995	1.000
Ballistic Transfer in Solar Max	3.91×10^{13}	9.86×10^{13}	2.11×10^{13}	0.995	0.985	1.000

In cislunar space, Moonraker will accumulate ionizing dose from solar radiation and GCRs at a rate of anywhere from 75% to 330% the rate it would accumulate in LEO, as illustrated in Fig. 8. When in low lunar orbit, the Moon blocks a significant portion of solar wind, reducing the ionizing dose rate. Therefore, the spacecraft will experience less ionizing dose from the Sun with decreasing altitude above the moon as shown in Fig. 9.

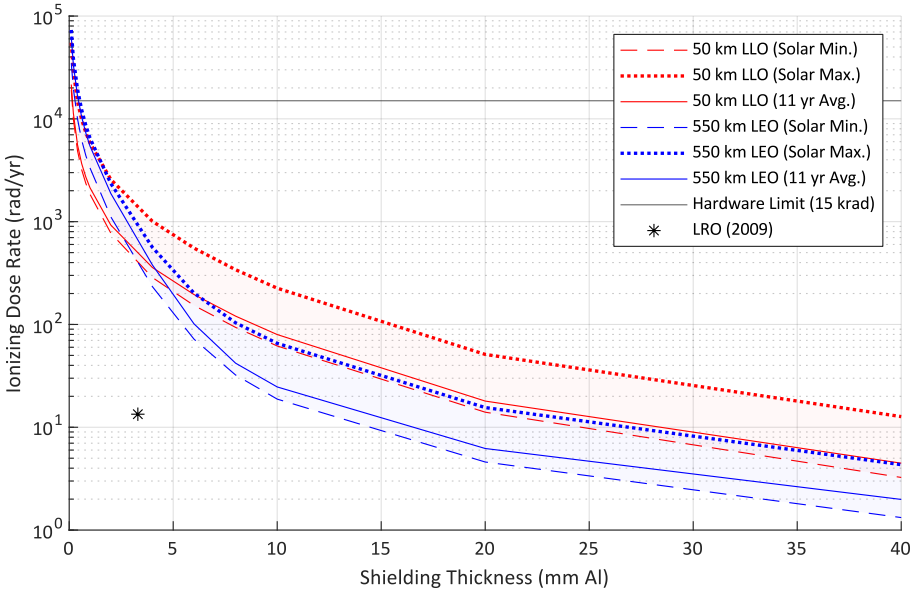

Fig. 8. Ionizing Does Rate vs. Shielding Thickness for a 50 km Operational Orbit

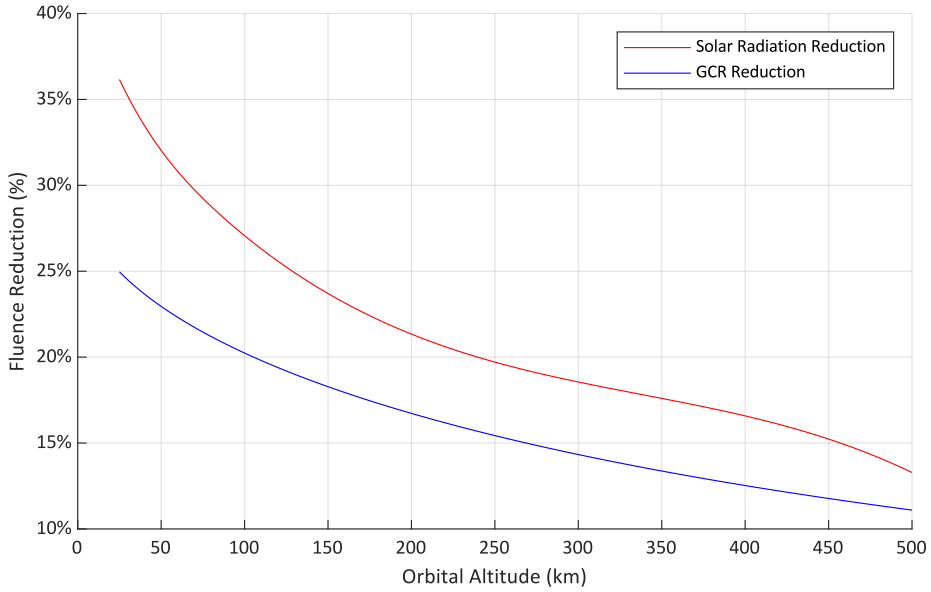

Fig. 9. Natural Radiation Shielding due to the Proximity of the Moon

Solar cells are expected to degrade at a faster rate in cislunar space when compared to LEO, due to the increased incidence of high-energy protons from the sun. Table 8 outlines the 11-year average rate of solar cell degradation in cislunar space and low Earth orbit. The yearly degradation factor in a low lunar orbit is only 0.2% worse than in LEO.

Table 8. Average Annual Solar Cell Degradation Rate in Cislunar Space and Low Earth Orbit

Location	1 MeV Equivalent Flux [e/cm^2]			Degradation Factor		
	P_{max}	V_{OC}	I_{SC}	P_{max}	V_{OC}	I_{SC}
Cislunar Space	2.33×10^{13}	5.87×10^{13}	1.26×10^{13}	0.997	0.991	1.000
Low Earth Orbit	4.36×10^{12}	1.09×10^{13}	2.39×10^{12}	0.999	0.998	1.000

The radiation environment for the possible lunar trajectories and operation at the Moon was analyzed. This analysis showed that all the transit trajectories are feasible with sufficient shielding. A bigger challenge will be the solar cell degradation experienced during the Earth-Moon L1 transit orbit trajectory. In this high radiation environment, solar cells with additional radiation hardening could be used or more of the same solar cells can be added to account for the reduced performance after the transfer is complete.

9. Spacecraft Concept Design

The Moonraker spacecraft concept design has been completed and is shown in Fig. 10. The Moonraker spacecraft interfaces with the launch vehicle via a 4-point separation system mounted on the launch vehicle interface panel on the -X face of the spacecraft. The primary thruster propellant tanks are all mounted to the bottom panel via composite tubing that attach to four tabs around the circumference of each tank. The four primary thrusters are mounted on the exterior of the bottom panel along with 4 of the 8 reaction control thrusters. The upper structure containing the payload, avionics, antennas, and the nitrogen tanks are mounted above the propellant tanks and supported by larger composite tubes. The panels on Moonraker are aluminum honeycomb core panels with carbon fiber face sheets to provide a stiff and mass efficient structure. These sandwich panels will include aluminum inserts imbedded into the core for mounting all components.

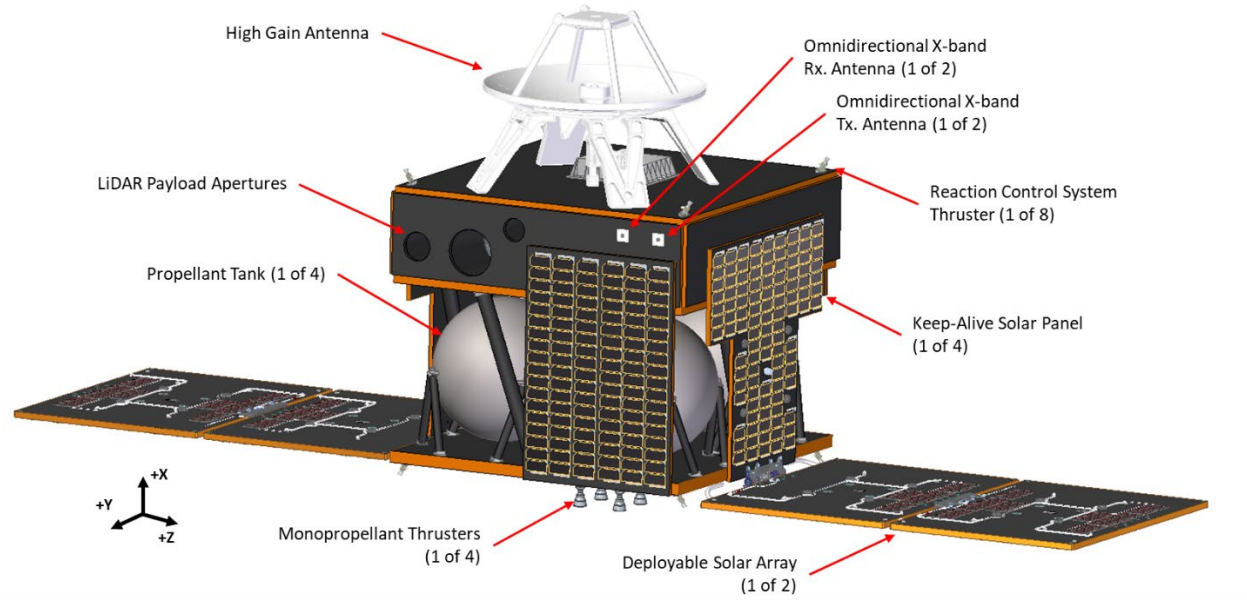

Fig. 10. The Moonraker Spacecraft in its Deployed Configuration

On the upper bus structure, the payload optics face outwards on the spacecraft. The high gain 0.75 m diameter dish antenna is mounted on the top of the spacecraft. The X-band receive and transmit patch antennas used for spacecraft recovery and back-up communication are located on the front and back. The pressurant tanks used as the reaction control system thruster propellant and the pressurant for the primary propulsion system, are mounted on the underside of the upper structure, in between the primary propellant tanks. All the RCS thrusters are tilted in the X-Z plane and are angled to ensure there is no plume impingement on any of the external components.

The keep-alive solar cells are mounted on lightweight sandwich panel coupons and are stood off from the structure to be thermally isolated from the bus. Four coupons are used on the sides of the spacecraft. The deployable solar arrays use the same sandwich panel construction as the rest of the structural panels. The deployables are held down with a hold-down release mechanism mounted on the inside of the coupon and constrained by 4 coup-cone interfaces. The Moonraker spacecraft will rely on a combination of body mounted solar cells and two deployable solar arrays for its power generation. The power generation will use two deployable solar arrays with each with 2 segments containing 8 strings of solar cells on one side with 6 additional strings on the bottom face for a total of 38 strings used for primary power generation.

The selected primary propulsion for Moonraker is a monopropellant system with four 22 N thrusters. The reaction control system uses eight 0.1 N cold gas thrusters. The thruster has a specific impulse of 242 s at a feed pressure of 18 bar. The propellant is stored in four diaphragm tanks with a propellant capacity of 45 L each. A pressurized system is used instead of a blowdown to maintain a constant thrust through the long maneuvers and to improve the end-of-life performance by keeping the propellant at 18 bar.

The spacecraft will include a high gain antenna with a 0.75 m diameter dish which will be used as the primary method of spacecraft telemetry, tracking, and command (TT&C) over X-band and payload data downlink over Ka-band. Moonraker will also be equipped with a set of omnidirectional X-band patch antennas that will be used as a back-up form of communication when the spacecraft is in safehold mode during initial commissioning, when recovering from a fault/reset, or during a loadshed event.

The spacecraft also has a suite of coarse attitude sensors using including 6 sun sensors and a rate sensor; that provide an attitude determination accuracy of about 2 degrees in sunlight. These sensors will only be used during early commissioning, and when recovering from a fault case. During fine pointing mode, the spacecraft will use 2 star trackers, mounted orthogonally to each other, to achieve a pointing knowledge of 7.9 arcsec (excluding thermal and structural misalignments). The spacecraft will use reaction wheels and reaction control thrusters for attitude control. The reaction control thrusters allow for detumbling following orbit insertion and momentum management for the wheels. A 4-wheel configuration is selected to avoid wheel zero-speed crossings during payload operations.

All of these sensors and actuators will be sampled and commanded by the spacecraft's guidance, navigation, and control computer. This computer runs SFL's 3-axis attitude control software called OASYS. At a high-level, OASYS is responsible for first taking in sensor measurements, and deriving an estimate of the spacecraft's state using an extended Kalman filter (EKF). This estimate is fed into the OASYS control algorithms, which compare the desired and estimated state, and use the difference between them to inform an actuation. The actuation commands are executed by the actuators, after which the control loop restarts.

Orbit determination and time reference updates will be provided via Earth ground station updates. The X-band transponder will capable of performing ranging and doppler measurements multiple times a day and at different locations to improve the orbit determination accuracy. Moonraker will be utilizing the GODOT flight dynamics software developed by ESA for orbital determination.

10. Conclusion and Future Work

The Moonraker spacecraft is nearing the end of its ESA funded Pre-Phase A study within the initiative on Small Missions for Exploration, and its inception "Destination the Moon". At this time, analyses and trade studies were performed to select the best trajectory for Moonraker to take to the Moon and what the operational orbit would be. The thermal and lunar environments during the transit to the Moon and in lunar orbit have been characterized for future design work. The spacecraft concept design has been completed by finalizing the structure layout, the propulsion and reaction control system selection, and selecting the avionics hardware for this mission.

Moonraker will look to build upon the work performed on the mission analysis and spacecraft concept design in the next phase of this ESA initiative. The payload optical design, structure, and thermal control strategy will be refined and the spacecraft will progress into the preliminary design phase. The development of the critical technologies required for a spacecraft operating in lunar orbit will continue and other components will be de-risked through thorough analysis, simulations, and testing. The Moonraker spacecraft, along with its LiDAR payload, will provide invaluable data in the form of digital elevation maps of the lunar terrain, especially at perspective landing sites for future lunar missions, and insight into the evolution of the Moon, which will help usher in a new age of lunar exploration.

Acknowledgements

We gratefully acknowledge the support of the European Space Agency who are funding the Pre-Phase A study for the Moonraker spacecraft. We appreciate the support and assistance of all the team members part of the consortium involved in this project including those from NUVIEW GmbH (the prime contractor of this consortium), DLR's Institute of Planetary Research, Lunar Outpost EU, AEM Antennas Inc., and KSAT.

References

[1] L. O. Magaña et al., “Surface roughness at the moon’s south pole: The influence of condensed volatiles on surface roughness at the moon’s south pole,” Planet. Sci. J., vol. 5, no. 2, p. 30, Feb. 2024.

[2] E. Belbruno, “Lunar capture orbits, a method of constructing earth moon trajectories and the lunar GAS mission,” in 19th International Electric Propulsion Conference, Colorado Springs,CO,U.S.A., 1987.

[3] P. Rathsman, J. Kugelberg, P. Bodin, G. D. Racca, B. Foing, and L. Stagnaro, “SMART-1: Development and lessons learnt,” Acta Astronaut., vol. 57, no. 2–8, pp. 455–468, Jul. 2005.

[4] S. K. Singh, R. Woollands, E. Taheri, and J. Junkins, “Feasibility of quasi-frozen, near-polar and extremely low-altitude lunar orbits,” Acta Astronaut., vol. 166, pp. 450–468, Jan. 2020.

[5] T. Nie and P. Gurfil, “Lunar frozen orbits revisited,” Celest. Mech. Dyn. Astron., vol. 130, no. 10, Oct. 2018.

[6] ESA Space Debris Mitigation Working Group, “ESA Space Debris Mitigation Requirements,” European Space Agency, 2023.

[7] C. Baker, M. Garrison, C. Cottingham, S. Peabody, D. Powers, T. Melak, “Lunar Reconnaissance Orbiter (LRO) Rapid Thermal Design Development,” presented at the Heatpipes for Space Applications International Conference, 2009.

[8] NASA, Human Landing System Lunar Thermal Analysis Guidebook, HLS-UG-01. NASA, 2021.

[9] National Institute of Standards and Technology, “Updated calculations for routine space-shielding radiation dose estimates:,” National Institute of Standards and Technology, Gaithersburg, MD, 1994.

[10] P. Jiggens et al., “The solar accumulated and peak proton and heavy ion radiation environment (SAPPHIRE) model,” IEEE Trans. Nucl. Sci., vol. 65, no. 2, pp. 698–711, Feb. 2018.

[11] R. A. Nymmik, M. I. Panasyuk, T. I. Pervaja, and A. A. Suslov, “A model of galactic cosmic ray fluxes,” Int. J. Radiat. Appl. Instrum. D Nucl. Tracks Radiat. Meas., vol. 20, no. 3, pp. 427–429, Jul. 1992.

[12] J. I. Vette, The NASA/National Space Science Data Center trapped radiation environment model program, 1964 - 1991, vol. 91, no. 29. National Aeronautics and Space Administration, Goddard Space Flight Center, 1991.